Defects in strained $In_{0.2}Ga_{0.8}As/GaAs$ multiple quantum wells on patterned and unpatterned substrates: A near-infrared cathodoluminescence study

D. H. Rich, K. C. Rajkumar, Li Chen,[a] and A. Madhukar[a]
Photonic Materials and Devices Laboratory, Department of Materials Science and Engineering, University of Southern California, Los Angeles, California 90089-0241

T. George, J. Maserjian, and F. J. Grunthaner
Center for Space Microelectronics Technology, Jet Propulsion Laboratory, California Institute of Technology, Pasadena, California 91109

A. Larsson
Chalmers University of Technology, Department of Optoelectronics and Electrical Measurements, S-412 96 Göteborg, Sweden

(Received 6 February 1992; accepted 20 March 1992)

The spatial distribution of the long-wavelength luminescence in thick $In_{0.2}Ga_{0.8}As/GaAs$ multiple quantum wells (MQWs) grown on patterned and unpatterned substrates has been investigated using cathodoluminescence (CL) imaging and spectroscopy. By spatially correlating the luminescence arising from the MQW exciton recombination ($\lambda \approx 950$ nm) with the longer wavelength ($1000 \lesssim \lambda \lesssim 1200$ nm) luminescence arising from the defect-induced recombination, we demonstrate that it is possible to determine the regions of highest film quality in both the mesa and valley regions for growth on patterned GaAs substrates. The present approach enables a judicious determination of the optimal regions to be used for active pixels in InGaAs/GaAs devices. For growth on unpatterned substrates, the CL spectra show defect-induced broad bands between $1000 \lesssim \lambda \lesssim 1600$ nm. These bands exhibit spatial variations which correlate with the dark line defects (DLDs) observed in the $\lambda = 950$ nm exciton luminescence imaging. Transmission electron microscopy showed that [110]-oriented misfit dislocations occur primarily at the substrate-to-MQW interface. The large spatial variation of the luminescence intensities indicates that the DLDs observed in CL images are caused by the presence of nonradiative recombination centers occurring in the MQW region located above the interface dislocations. This study provides new information describing the origin and nature of DLDs and differs from previous models, which have regarded the electronic nature of dislocation cores as the primary mechanism for inducing DLD radiative contrast in luminescence imaging of strained InGaAs/GaAs.

I. INTRODUCTION

Presently, there is a considerable interest in using selective-area epitaxial growth approaches to achieve the fabrication of thick coherent films of strained InGaAs and related multiple quantum well structures (MQW) structures on GaAs substrates. Many applications in the area of optical computing, communication, and detection will benefit from the continuing advancements made in the molecular-beam epitaxial (MBE) growth techniques of highly strained InGaAs films. Previous studies employing transmission electron microscopy (TEM),[1-4] photoluminescence (PL),[2,5] cathodoluminescence (CL),[6] optical absorption,[1,3] and micro-Raman,[4] have demonstrated a substantial reduction in the density of misfit dislocations occurring in thick $In_xGa_{1-x}As$ films and MQWs grown on GaAs mesas with dimensions between 1 and 400 μm.

The technique of CL microscopy enables the measurement of luminescence behavior with a scale of approximately micron or less; this is quite valuable for the optical characterization of III–V semiconductor device arrays having active pixels with such dimensions. The spatial distribution of the near-infrared ($900 \lesssim \lambda \lesssim 1600$ nm) luminescence in thick $In_{0.2}Ga_{0.8}As/GaAs$ MQWs grown on patterned and unpatterened substrates has been examined with CL imaging and spectroscopy. We show that by spatially correlating the luminescence arising from electron-to-heavy hole (e-hh) exciton recombination in the MQWs with the longer wavelength luminescence arising from the defect-induced recombination, it is possible to determine the regions of highest film quality in both the mesa and valley regions for patterned InGaAs/GaAs MQW structures. The effects of cation migration near faceted sidewalls of chemically etched rectangular mesas are examined.

For growth of MQWs on unpatterned substrates, the long-wavelength luminescence features are found to correlate spatially with the dark line defects (DLDs) seen in the imaging of the MQW exciton recombination at $\lambda \approx 950$ nm. Plan-view and cross-sectional TEM show that misfit dislocations in the samples are confined to the region near the interface. The luminescence intensities from various MQW structures are quantified, and a large variation in intensity of the luminescence associated with the DLDs suggest that most of the QWs in the vicinity of the DLDs are affected by the misfit dislocations. This intensity vari-

 0734-211X/92/041965-06$01.00

ation is found to be relatively independent of the electron beam probing depth, and indicates that the QWs are affected homogeneously throughout all the layers, in contrast to the presence of misfit dislocations which occur *only* at the MQW-to-substrate interface. This luminescence behavior is attributed to a relative increase in the number of *nonradiative* recombination centers occurring in regions above the interface dislocations. These results suggest that nonradiative point defects above the interface dislocations are left in the wake of dislocation propagation and multiplication. In the Si system Kimerling and co-workers,[7] using deep-level transient spectroscopy, have speculated that it is the point defects gettered around dislocations which are largely responsible for defect induced midgap states and the associated recombination properties. Similarly, we demonstrate that a Cottrell atmosphere of point defects surrounding dislocations is the most reasonable explanation for the DLD behavior observed in this study of $In_{0.2}Ga_{0.8}As/GaAs$ MQW structures.

II. EXPERIMENT

MQW samples were grown by MBE using standard In, Ga, and As sources. Our study of growth on unpatterned substrates involves 65 Å thick $In_{0.2}Ga_{0.8}As$ QWs surrounded by GaAs barriers. In samples designated D92, D18, and D38, 44 periods of $In_{0.2}Ga_{0.8}As$ MQWs were grown with barrier thicknesses of 780, 400, and 115 Å, respectively. In sample D179, a 65 Å MQW structure having 100 and 1230 Å barriers with 14 periods (28 QWs) were grown. A control sample, D155, was grown with one 65 Å thick QW. One of the samples, D92, was periodically δ doped; Be and Si doping planes with concentrations of 9.0×10^{12} and 3.0×10^{12} cm^{-2} were inserted at the centers and 290 Å off centers of the GaAs barriers to produce a *nipi* effect. This sample was grown originally for the purpose of studying suitable structures for optically addressed spatial light modulators.[8] The spatial separation of electrons and holes enables a large optically induced absorption modulation for this structure; this has been recently reported.[8,9] For patterned growth, a n^+-type GaAs(100) substrate was patterned using conventional optical lithography and wet chemical etching.[1–3] The crystallographically selective etch results in undercut and inclined sidewall planes [mostly {111} with some high index facets] at the mesa edges. The resulting mesas had dimensions of about 2 μm thick $\times$ 16 μm $\times$ 18 μm with a 40 μm spacing in both directions before MBE growth. A scanning electron micrograph (SEM) image of a typical mesa is shown in Fig. 1. About half the wafer was left unpatterned in order to allow for examination of a reference sample. The structure grown on top consisted of a 100 period $In_{0.2}Ga_{0.8}As$ (80 Å)/GaAs(160 Å) MQW (having $\sim$2.38 μm total thickness) with a 5000 Å p^+-type GaAs capping layer. Cross-sectional TEM (XTEM) and absorption results of this sample (designated RG891110) have been previously described.[1,3] CL measurements were performed with a JEOL 840-F field-emission SEM at the Jet Propulsion Laboratory.[10] A North Coast E0-817L Ge *p–i–n* detector was used to measure the signal dispersed by a 0.25 m monochromator. An electron beam current of 0.5 nA at accelerating voltages ranging from 10 to 40 kV was used to probe the sample for the CL measurements. The sample was maintained at a temperature of $\sim$77 K.

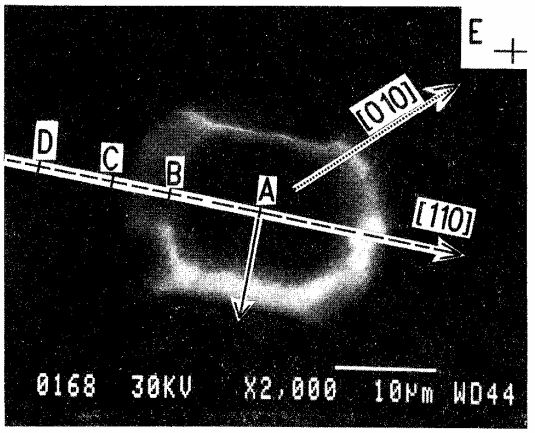

FIG. 1. SEM of a typical mesa of the $In_{0.2}Ga_{0.8}As/GaAs$ MQW structure. The dashed and solid lines with arrows oriented along [110] and [1$\bar{1}$0], respectively, indicate the position of the electron beam during line scans. Points A–E indicate beam position during local CL spectroscopy.

III. RESULTS AND DISCUSSION

A. $In_{0.2}Ga_{0.8}As$ growth on patterned GaAs(100)

A SEM image of the structure showing a 220 μm $\times$ 170 μm area is presented in Fig. 2(a). Scanning monochromatic CL images corresponding to the same region are shown in Figs. 2(b)–2(d) for wavelengths of 950, 1040, and 1120 nm, respectively. Regions of increasing luminescence signal are represented by areas of lighter shades. The image with $\lambda = 950$ nm [in Fig. 2(b)] shows a hatched region of bright luminescence with maximum intensity in the valley regions midway along the [010] diagonal (dotted line in Fig. 1) between mesa centers. There is some observable emission from the centers and edges of the mesas at this wavelength. A dark halo region is found to surround the mesas, where little emission is detected. As the wavelength is increased to 1040 and 1120 nm, the images in Fig. 2 show an enhanced emission from the centers and sides of the mesas relative to the valley regions. Also, for these wavelengths (and for other CL imaging wavelengths in the region $1000 \leqslant \lambda \leqslant 1200$ nm not shown here), the luminescence patterns on top of most of the mesas show a distinct dumbbell shape with maximal intensity near the mesa edges parallel to [1$\bar{1}$0], as seen in Figs. 2(c) and 2(d). The dumbbell shape on the mesas, as seen in the $\lambda \geqslant 1000$ nm CL images and the [110] CL line scan, indicates the presence of interfacet cation migration in which the In migrates up along the inclined edges. The presence of contiguous low index planes is known to cause interfacet migration; this behavior has been observed to cause compositional variations in the AlGaAs and InGaAs films grown on patterned substrates.[1–3,5,11]

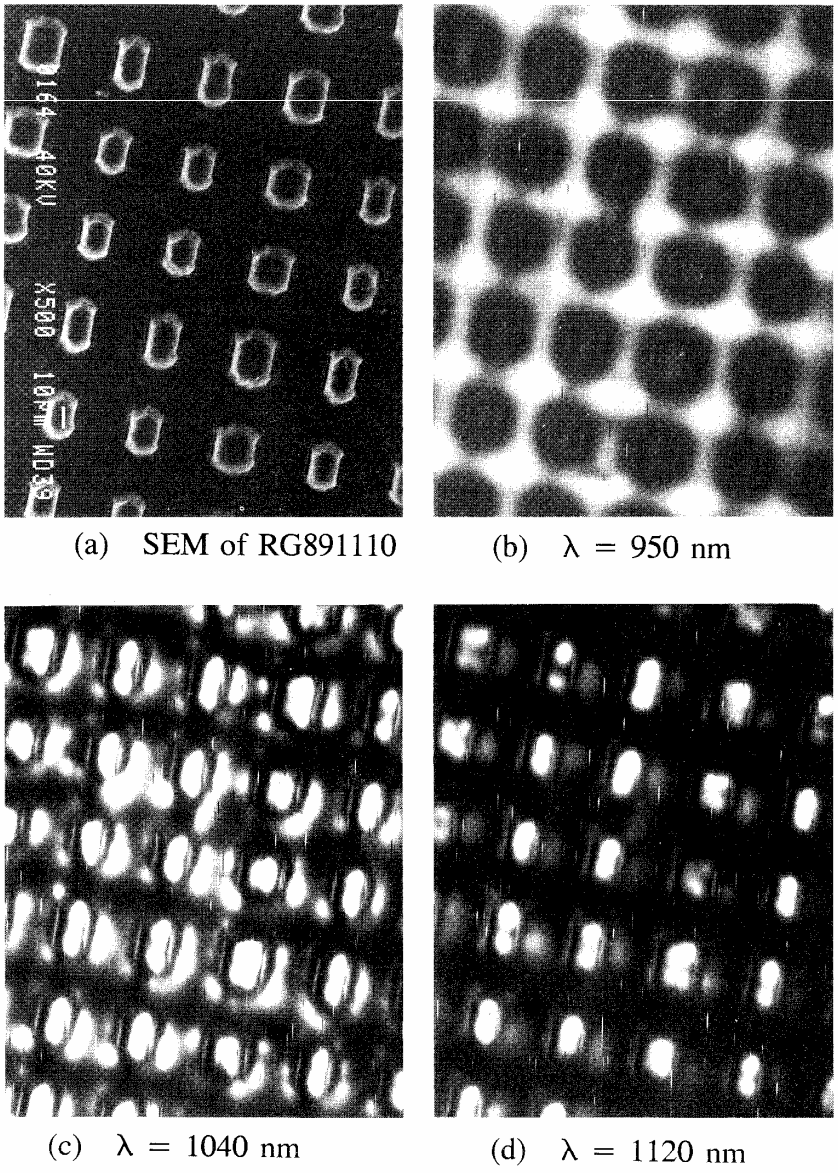

FIG. 2. SEM (a) and scanning monochromatic cathodoluminescence images [(b), (c), and (d) correspond to wavelengths of 950, 1040, and 1120 nm, respectively] of the same region of the $In_{0.2}Ga_{0.8}As/GaAs$ MQW structure.

Previously, TEM measurements of the mesa region for RG891110 has shown that the linear defect density to be less than $\sim 10^5$ cm^{-1}.[1] Since the maximum spatial resolution in CL is limited by the carrier diffusion length (~ 1 μm for GaAs), we do not expect to see the effects of individual dislocations. It will be shown below (in Sec. III B) that for the D-series unpatterned samples, the presence of underlying misfit dislocations at the MQW-to-substrate interface gives rise to a crosshatched pattern when the linear defect density is less than $\sim 10^4$ cm^{-1}.

Localized CL spectra are shown in Fig. 3; locations A–E correspond to points on a mesa center, mesa edge, valley region near mesa, midway between mesas along [110], and midway between mesas along [010], respectively, as labeled in Fig. 1. The spectrum labeled Ref. corresponds to an unpatterned region and does not exhibit a measurable exciton luminescence. The peak at $\lambda = 950$ nm corresponds to the e-hh exciton luminescence. The regions exhibiting the largest defect-induced luminescence ($1000 \lesssim \lambda \lesssim 1200$ nm) on the mesa are found in close proximity to the inclined regions at the mesa edges (position B in Fig. 1) which result from the crystallographic selectivity

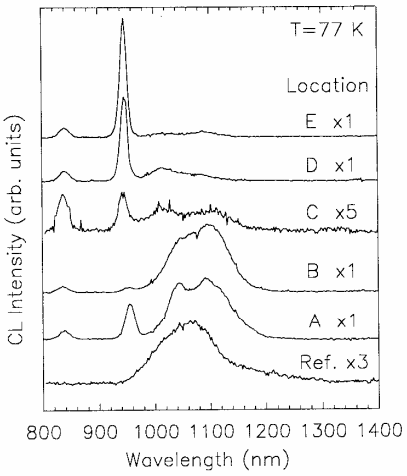

FIG. 3. Localized CL spectroscopy at the points A–E shown in Fig. 1. The sample labeled Ref. corresponds to the spectrum taken in the nonpatterned region of the $In_{0.2}Ga_{0.8}As/GaAs$ MQW structure.

of the etch. The region possessing the highest film quality has been determined by measuring the exciton-to-defect emission ratio for a variety of positions in the structure. The data show, surprisingly, that the highest-quality film exists in the valley regions which are midway between the mesa centers (location E in Fig. 1) and not at the mesa centers (location A in Fig. 1). These results are expected to influence current thinking with regard to the design and processing of pixelated devices.

B. Growth of $In_{0.2}Ga_{0.8}As$ on unpatterned GaAs(100)

TEM was performed on the D38, D18, D92, and D179 samples. The MQW regions showed well-ordered $In_{0.2}Ga_{0.8}As$ and GaAs which were visibly free of structural defects. Only at and below the MQW-to-substrate interface did there appear to be disorder in the form of interface misfit dislocations and looping dislocations that propagated into the GaAs substrates. Furthermore, by progressively thinning away the back side of the substrates, we determined, using plan view TEM, that the misfit dislocation cores were confined soley to the MQW/GaAs interfacial region.

CL images of D38, D18, D92, D155, and D179 are shown in Figs. 4(a)–4(e). The wavelength used for the imaging was $\lambda \approx 950$ nm and corresponds to the e-hh transition in the MQW samples. The DLDs are evident in each of the images except for D155, the single QW sample [Fig. 4(d)]. The absence of misfit dislocations in the single QW sample is to be expected since the nominal critical thickness of a single $In_{0.2}Ga_{0.8}As$ layer grown on GaAs(100) is ~ 150–200 Å.[12] These images showing DLDs here are similar to luminescence images of thick InGaAs films previously studied.[6]

In order to further assess the luminescence properties, we examined CL spectra of the unpatterned InGaAs samples in the wavelength range $900 \lesssim \lambda \lesssim 1600$ nm. The spectra (not shown here) are similar to that shown in Fig. 3 for the growth on the patterned substrates; four distinct features in the luminescence were observed centered at 950, 1250, 1380, and 1460 nm. The peak at $\lambda = 950$ nm is the e-hh transition. Joyce *et al.*,[13] using PL, have observed emission in the $1000 \lesssim \lambda \lesssim 1600$ nm range for thick InGaAs films grown on GaAs. These emissions were found to in-

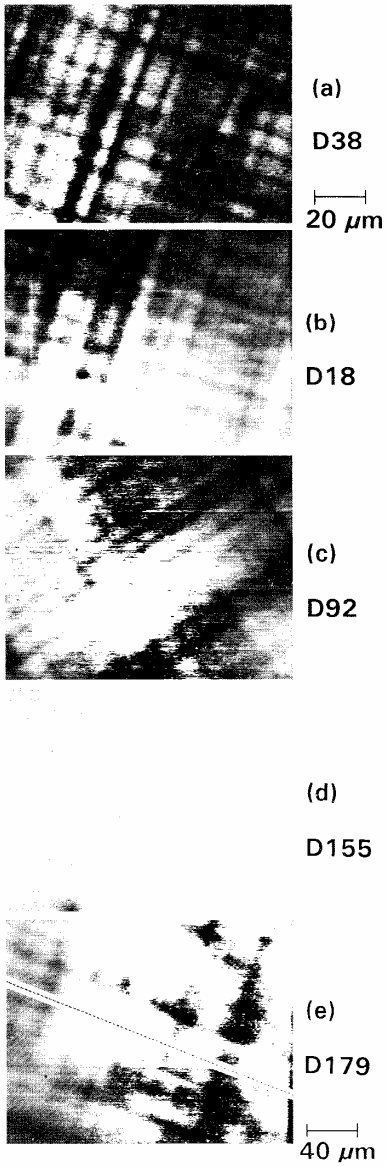

FIG. 4. Scanning monochromatic CL images of the e-hh exciton luminescence for $\lambda \approx 950$ nm. The sample number and MQW structure are described in (a)–(e). The 20 μm scale indicated in (a) also represents the scale for (b)–(d); note the factor of 2 scale change in (e). A dashed line along [110] in (e) indicates the electron beam path during the line scan measurements performed for D179.

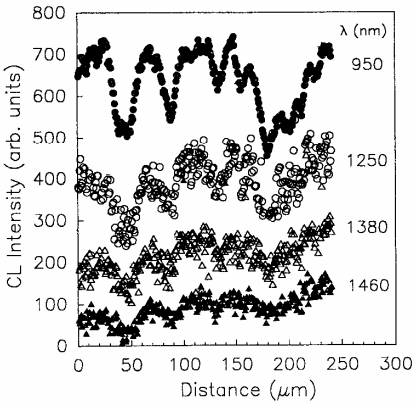

FIG. 5. CL line scans (intensity vs position histogram) for MQW sample D179. The electron beam position is indicated in Fig. 4(e). The peaks and valleys in the $\lambda = 950$ nm scan of the e-hh exciton luminescence correlates with the peaks and valleys of the longer wavelength 1250, 1380, and 1460 nm scans.

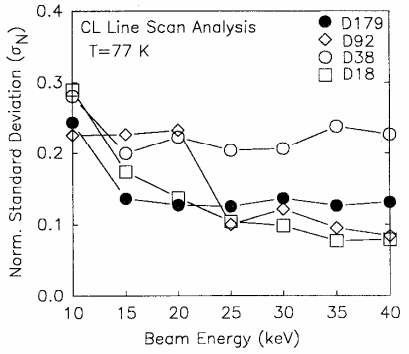

FIG. 6. The normalized standard deviation (σ_N) of the e-hh exciton luminescence line scans for MQW samples. The standard deviation has been normalized to the mean of the exciton luminescence for each line scan. The large magnitude of the variation (see discussion) precludes the possibility of only one QW in each structure being affected by a single dislocation core at the MQW-to-substrate interface.

crease markedly when the $In_{0.17}Ga_{0.83}As$ layer thicknesses exceeded the critical thickness, and Joyce *et al.* concluded that this behavior was due to an increase in interface defects, such as misfit dislocations, beyond the critical thickness.[13] In order to test this hypothesis, we have determined the spatial distribution of all distinct emissions in the wavelength range $900 \lesssim \lambda \lesssim 1600$ nm. We have measured intensity versus position histograms or line scans (see Fig. 5) which quantitatively give the spatial variation in luminescence intensity for the different wavelengths. The line scans for wavelengths of 1250, 1380, and 1460 nm have essentially the same spatial variation as the $\lambda = 950$ nm scan, i.e., peaks and valleys in the longer wavelength scans correspond with peaks and valleys in the $\lambda = 950$ nm scan. This is a surprising result since, from Ref. 12, we would expect the region around the DLDs to yield an enhanced emission rather than the reduced emission at longer wavelengths.

The nature of the dislocation cores (i.e., electronic structure and reconstruction) in strained III–V materials is known to effect the recombination process. The studies of Fitzgerald *et al.*[6] and Petroff *et al.*[14] on strained films have shown that 60° dislocations and edge dislocations have different nonradiative recombination rates in the vicinity of these dislocations. It is apparent from the data of Fig. 5 that the nonradiative mechanisms responsible for the reduction in the e-hh exciton luminescence are also responsible for reduction in the $1000 \lesssim \lambda \lesssim 1600$ nm emissions. This results in longer wavelength DLDs spatially correlated with the conventional e-hh exciton DLDs. The origin of the $1000 \lesssim \lambda \lesssim 1600$ nm emissions is, evidently, not *directly* caused by the presence of misfit dislocations and may be due to the presence of point defects. Similar broad and midgap emissions have been observed in thick and heavily strained GaAs films grown on Si which are believed to contain interstitial, antisite, and vacancy defects.[15] In addition, we can not rule out emissions due to the presence of $In_{0.2}Ga_{0.8}As/GaAs$ interfaces (i.e., recombinations involving interface states). Other types of structural defects can also induce midgap emissions. A particularly striking result in Fig. 5 is the large intensity variation seen in the line scan data. The variation of the luminescence in the $\lambda = 950$ nm line scans can be quantified by evaluating the standard deviation of all points shown in a line scan, and normalizing the standard deviation with respect to the mean. In order to reduce the uncertainties due to variation in the signal-to-noise caused by changes in the luminescence signal associated with changing the excitation conditions (current and beam energy) and different sample thicknesses, a cubic spline fit was used to determine the "smooth curve" through each line scan. The normalized standard deviation σ_N of fitted $\lambda = 950$ nm line scans are shown in Fig. 6 for all samples with a beam energy ranging from 10 to 40 keV. A general trend is observed in which σ_N is fairly constant over a large energy range and increases slightly with a decreasing probing depth for energies less than about 20 keV. The total thicknesses of the MQW region of D179, D92, D38, and D18 are 2.0, 3.7, 0.8, and 2.0 μm, respectively, and a given variation in the probing depth will affect different regions of each sample. From the above TEM results, we know that misfit dislocations occur only in the region at the MQW-to-substrate interface. We should expect, therefore, that only recombination in the QW closest to the interface will be disturbed directly by the presence of a misfit dislocation. A predicted σ_N for a 44 MQW structure in which the luminescence from one QW at the interface is completely suppressed by a misfit dislocation, assuming a homogenous carrier excitation and a simple sinusoidal spatial variation in the luminescence, is $\sigma_N = 0.008$. This is at least an order of magnitude too low to explain the present results of Fig. 6. Instead the magnitude of σ_N and its relative constancy for each sample in Fig. 6 suggest that the nonradiative mechanisms giving rise to DLDs are spread homogeneously throughout all MQWs in each sample, and the effects become slightly more pro-

nounced for more surface sensitive probing conditions.

These results have significant ramifications concerning the origin of the DLDs seen in this and previous studies of thick InGaAs films grown on GaAs. In previous studies, it was simply assumed that the electronic nature of the misfit dislocations were responsible for the creation of competing nonradiative channels.[6,14] In that model, nonradiative minority carrier recombination occurs at the reconstructed dislocation cores as a result of localized band bending in the vicinity of the cores; the density of defect-induced states in the band gap and doping concentration will determine local depletion region sizes. However, the present data suggest that carrier recombination at the dislocation cores is a minor effect in producing the DLDs observed in CL. This can be proven immediately by considering the *nipi* structure of sample D92. The modulation doping will cause electrons and holes to spatially separate for carriers which do not recombine at the location of the $In_{0.2}Ga_{0.8}As$ QWs, and this results in negligible carrier diffusion along the [100] growth direction.[8,9] Therefore, it is apparent that recombination of carriers which are generated more than one MQW period away from the dislocation core would be negligible in this model. The only reasonable explanation for the behavior of σ_N is as follows. The existence of nonradiative recombination centers spread homogeneously in the MQW material above the dislocations is the primary cause for the large variation in the MQW exciton luminescence. The nonradiative centers will evidently compete with the longer wavelength $1000 \lesssim \lambda \lesssim 1600$ nm radiative channels, resulting in the spatial correlation of DLDs imaged at $\lambda \approx 950$ nm with DLDs imaged at longer wavelengths (as illustrated in Fig. 5 for line scans). Dislocation propagation and multiplication such as, e.g., the Hagen–Strunk[16] and surface half-loop nucleation[17] mechanisms are expected to disturb the material located above the dislocations. Heavily dislocated materials, such as that seen in the strained GaAs/Si system are known to contain a significant density of point defects.[7,15] It is, therefore, likely that a "Cottrell atmosphere" of point defects left in the wake of dislocation propagation and multiplication coupled with the concomitant expitaxical growth over the vicinities of such propagation are responsible for the observed behavior of σ_N.

ACKNOWLEDGMENTS

The research described in this article was performed by the Center for Space Microelectronics Technology, Jet Propulsion Laboratory, California Institute of Technology, and was jointly sponsored by the Defense Advanced Research Projects Agency, the Strategic Defense Initiative Organization, Innovative Science and Technology Office, and the National Aeronautics and Space Administration, Office of Aeronautics, Exploration, and Technology. At USC, part of this work was supported by AFOSR, URI (AFOSR), DARPA, and ONR.

[a] Also with the Department of Physics.
[1] A. Madhukar, K. C. Rajkumar, L. Chen, S. Guha, K. Kaviani, and R. Kapre, Appl. Phys. Lett. **57**, 2007 (1990).
[2] S. Guha, A. Madhukar, and L. Chen, Appl. Phys. Lett. **56**, 2304 (1990).
[3] L. Chen, K. Hu, K. C. Rajkumar, S. Guha, R. Kapre, and A. Madhukar, *Proceeding of the Materials Research Society Symposium on Materials for Optical Information Processing,* Anaheim, CA, May 1–3, 1991 (in press).
[4] W. C. Tang, H. J. Rosen, S. Guha, and A. Madhukar, Appl. Phys. Lett. **58**, 1644 (1991).
[5] Y. Zou, P. Grodzinski, J. S. Osinski, and P. D. Dapkus, Appl. Phys. Lett. **58**, 717 (1991).
[6] E. A. Fitzgerald, G. P. Watson, R. E. Proano, D. G. Ast, P. D. Kirchner, G. D. Pettit, and J. M. Woodall, J. Appl. Phys. **65**, 2220 (1989), and references therein.
[7] L. C. Kimerling and J. R. Patel, Appl. Phys. Lett. **34**, 73 (1979); G. L. Miller, D. Lang, and L. C. Kimerling, Annu. Rev. Mater. Sci. **7**, 377 (1977); L. C. Kimerling, Mater. Res. Soc. Bull. **16**, 42 (1991).
[8] A. Larsson and J. Maserjian, Appl. Phys. Lett. **58**, 1946 (1991).
[9] J. Maserjian, P. O. Andersson, B. R. Hancock, J. M. Iannelli, S. T. Eng, F. J. Grunthaner, K.-K. Law, P. O. Holtz, R. J. Simes, L. A. Coldren, A. C. Gossard, and J. L. Merz, Appl. Opt. **28**, 4801 (1989).
[10] D. II. Rich, A. Ksendzov, R. W. Terhune, F. J. Grunthaner, B. A. Wilson, H. Shen, M. Dutta, S. M. Vernon, and T. M. Dixon, Phys. Rev. B **43**, 6836 (1991).
[11] For migration in AlGaAs, see, e.g., S. Guha, A. Madhukar, K. Kaviani, L. Chen, R. Kuchibhotla, R. Kapre, M. Hyugaji, and Z. Xie, Mater. Res. Soc. Proc. **145**, 27 (1989).
[12] S. Luryi and E. Suhir, Appl. Phys. Lett. **49**, 140 (1986).
[13] M. J. Joyce, M. Gal, and J. Tann, J. Appl. Phys. **65**, 1377 (1989).
[14] P. M. Petroff, R. A. Logan, and A. Sauvage, Phys. Rev. Lett. **44**, 287 (1980); J. Microsc. **118**, 255 (1980).
[15] B. A. Wilson, C. E. Bonner, T. D. Harris, M. G. Lamont, R. C. Miller, S. K. Sputz, S. M. Vernon, V. E. Haven, R. M. Lum, and J. K. Klingert, Mater. Res. Soc. Symp. Proc. **91**, 255 (1987). Additionally, in a stress-induced deformation of Si and Ge samples, Schröter, Scheibe, and Schoen [J. Microsc. **118**, 23 (1980)] have argued that variations in the mobility and density of free holes, as determined from Hall measurements, are associated with clouds of point defects which surround dislocations.
[16] W. Hagen and H. Strunk, Appl. Phys. **17**, 85 (1978).
[17] J. W. Matthews, A. E. Blakeslee, and S. Mader, Thin Solid Films **33**, 253 (1976).